Physical Properties of a New Type of Molten Electrolytes, $FeCl_3$-$DMSO_2$

Chao-Chen Yang[a] and Min-Fong Shu[b]

[a] Department of Environmental Resources Management, Overseas Chinese Institute of Technology, Taichung, Taiwan, R.O.C.
[b] Graduate School of Engineering Science and Technology (Doctoral Program), National Yunlin University of Science and Technology. 123, Sec. 3, University Road, Touliu, Yunlin, Taiwan, R.O.C.

Reprint requests to C.-C. Y.; Fax: 886-5-531-2071; E-mail: president@ocit.edu.tw.

Z. Naturforsch. **60a,** 444 – 448 (2005); received November 11, 2004

Some physical properties of ferric chloride-dimethyl sulfone ($FeCl_3$-$DMSO_2$) melts were investigated. The phase diagram was determined by differential scanning calorimeter and thermogravimetric analyzer. The electric conductivity, measured with computerized direct-current method, increased with increasing temperature and $DMSO_2$ content. The conductivity was maximal (0.02149 S/cm) at 115 °C for 30 mol% $FeCl_3$. The densities of all melts decreased with increasing temperature and $DMSO_2$ content. The equivalent conductivities were given by $\Lambda = \kappa M_{mix}/\rho$, where M_{mix} is the mean equivalent weight of the binary melts. These equivalent conductivities were fitted by the equation $\Lambda = \Lambda_0 \exp(-E_\Lambda/RT)$, where the activation energies E_Λ were 8.63, 22.94, 25.92 kJ/mol for 30, 40, 50 mol% $FeCl_3$, respectively.

Key words: Computerized Direct-current Method; Equivalent Conductivity; Activation Energy.

1. Introduction

Molten salt systems with high conductivities have extensively been studied for the development of molten salt techniques, such as electrodeposition of alloy metals, codeposition of silica particles, electrolytes for secondary batteries, and plating magnetic data storage materials. Research on room temperature molten salts (RTMS) has drawn considerable attention [1, 2].

Hsu and Yang [3] have reported the conductivities of the binary systems $AlCl_3$-$C_9H_{14}ClN$ (*N-n*-butylpyridinium chloride, BPC), $AlCl_3$-$C_6H_{11}ClN_2$ (1-ethyl-3-methyl-imidazolium chloride, EMIC) and $AlCl_3$-$C_{13}H_{22}ClN$ (benzyltriethylammonium chloride, BTEAC). Some new melts have been prepared by adding inorganic salts to organic solvents, e.g. $AlCl_3$-$DMSO_2$ [4] and $ZnCl_2$-$DMSO_2$ [5]. It was shown that $DMSO_2$ is a good solvent, stable at high temperature and able to dissolve numerous metallic salts. Yang et al. [6 – 8] have studied the electrodeposition of Zn, Dy, Zn/Pd and Co/Al alloys from $ZnCl_2$-EMIC and $AlCl_3$-BPC melts. However, neither the conductivity nor the density of melts containing $DMSO_2$ as solvent has been reported.

2. Experimental

2.1. Chemicals

$FeCl_3$ (ferric chloride, Riedel de Haën, anhydrous, 98%) and $DMSO_2$ (dimethylsulfone, Acros, 98%) were used in a dry glove box with a nitrogen atmosphere. The nitrogen had been passed through a drying column containing molecular sieves. The solutions were prepared in the dry glove box by mixing the $DMSO_2$ with appropriate amounts of $FeCl_3$ at 90 °C on a hot plate with a silicone oil bath.

2.2. Phase Diagram

The phase diagram of the $FeCl_3$-$DMSO_2$ melts was obtained by measuring the decomposition temperatures and the melting points. The thermal analyses were performed by TGA and DSC; the data of the thermal analyses are shown in Figure 1. The TGA analyses of the binary melts were carried out on a platinum tray which could be heated from 35 to 500 °C with a heating rate of 20 K/min. For the DSC analysis a sealed aluminum disc was used, which was cooled down to −60 °C by liquid nitrogen and then heated at a rate of 10 K/min.

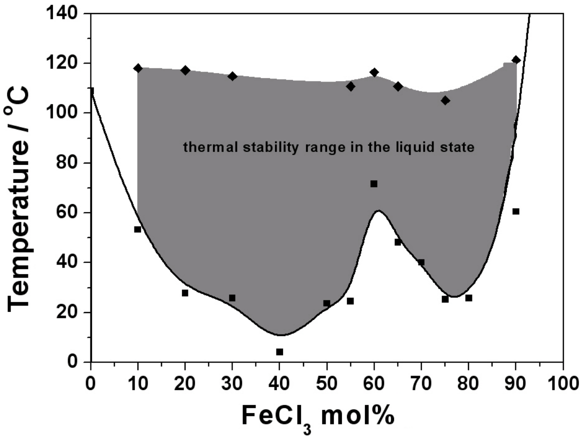

Fig. 1. Phase diagram of $FeCl_3$-$DMSO_2$.

2.3. Density

The density was measured, using the Archimedean principle [9–11], by determining the buoyancy of a platinum hammer immersed in the melt, which was suspended by a platinum wire (0.2 mm diameter) from one arm of a precise analytical balance (Mettler Toledo, AT261 DeltaRange), the apparatus being schematically shown in [6]. The volume of the hammer was 2.4 cm^3.

2.4. Conductivity

The conductivity was determined by a computerized direct-current method [3, 5]. The cell constant, calculated with a 0.1 demal KCl solution at 25 °C, was 302.25 cm^{-1}. The reference electrodes were an Ag-AgCl electrode and a platinum electrode. A direct current (Hewlett-Packard E3616A) of 2.5 A passed the Pt electrodes. Two multimeters (Keithley, Model 2000) were employed for determining the potential drop at the two platinum electrodes.

3. Results and Discussion

The phase diagram is shown in Figure 1. The decomposition temperatures were measured by the TGA analysis and the melting points by the DSC analysis. The two lowest melting points were 4.14 °C at 40 mol% $FeCl_3$ and 25.19 °C at 76 mol% $FeCl_3$.

Densities of molten $FeCl_3$-$DMSO_2$ vs. the temperature are shown in Figure 2. When the density are approximated by linear functions $\rho = a' - b't$ of the temperature t in °C, a' and b' result as given in Table 1.

Table 1. Densities of molten $FeCl_3$-$DMSO_2$.

$FeCl_3$	$\rho = a' - b't$		R-squared	Temp. range
	a'	b'		
mol%	10^{-4} g cm^{-3}	g cm^{-3} °C^{-1}		°C
20	7.625	1.301	0.97756	81 – 115
30	7.019	1.358	0.99865	81 – 115
40	9.075	1.446	0.99721	81 – 115
50	8.276	1.499	0.99883	81 – 115

Table 2. Molar volumes of molten $FeCl_3$-$DMSO_2$.

$FeCl_3$	$V = a'' + b''t$		R-squared	Temp. range
	a''	b''		
mol%	10^{-2} cm^3 mol^{-1}	cm^3 mol^{-1} °C^{-1}		°C
20	4.354	65.914	0.97910	81 – 115
30	3.464	60.274	0.99877	81 – 115
40	3.845	53.780	0.99763	81 – 115
50	3.047	49.260	0.99915	81 – 115

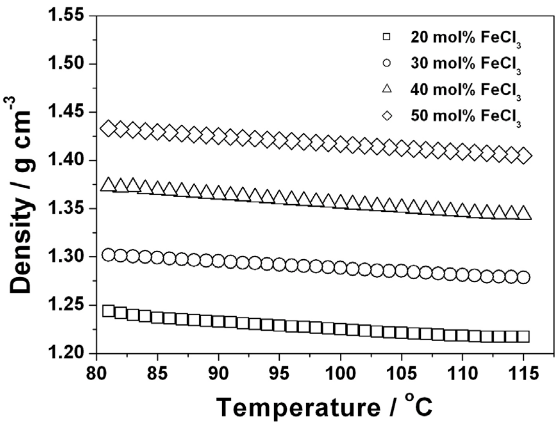

Fig. 2. The density of $FeCl_3$-$DMSO_2$ melts vs. the temperature at 20, 30, 40, and 50 mol% $FeCl_3$.

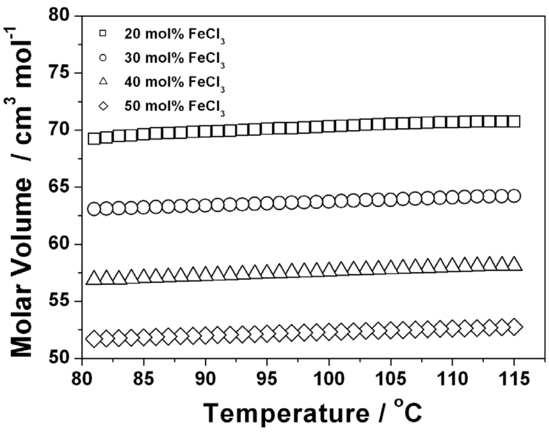

Fig. 3. The molar volume of $FeCl_3$-$DMSO_2$ melts vs. the temperature at 20, 30, 40, and 50 mol% $FeCl_3$.

$FeCl_3$	$\kappa = a + bt + ct^2$			R-squared	Temp. range
	a	b	c		
mol%	10^{-3} S cm^{-1}	10^{-4} S cm^{-1} °C^{-1}	10^{-7} S cm^{-1} °C^{-2}		°C
30	−21.84	5.70	−16.88	0.99498	81 – 115
40	7.6	−1.45	19.87	0.99763	81 – 115
50	−12.22	2.45	−4.407	0.99746	81 – 115
75	−12.73	2.53	−8.71	0.98583	81 – 115

Table 3. Electric conductivities of molten $FeCl_3$-$DMSO_2$.

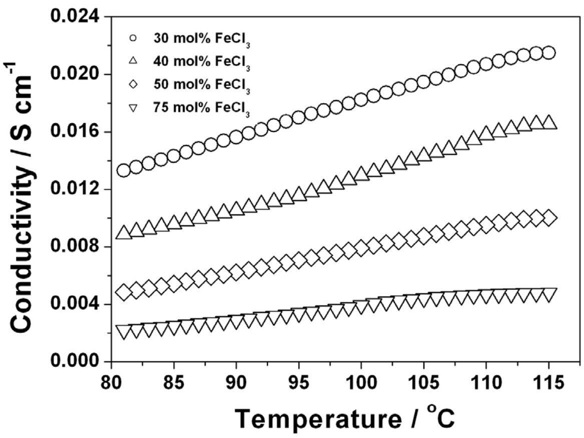

Fig. 4. The electric conductivity of $FeCl_3$-$DMSO_2$ melts vs. the temperature at 30, 40, 50, and 75 mol% $FeCl_3$.

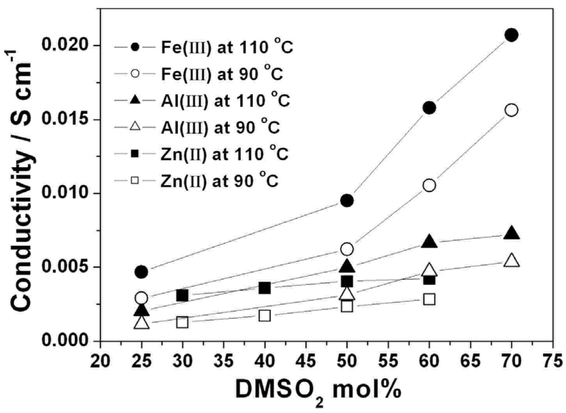

Fig. 5. Isotherms of the electrical conductivity vs. the mole fraction of $DMSO_2$ for the molten binary systems $ZnCl_2$-$DMSO_2$, $AlCl_3$-$DMSO_2$, and $FeCl_3$-$DMSO_2$ at 90 and 110 °C.

Corresponding molar volumes are shown in Fig. 3 and the linear approximation given in Table 2. The density could be influenced by complexing of the molecules or efficient packing of the ions [9].

The relationship between electric conductivity and temperature at various compositions is shown in Figure 4. The experimental data were fitted to equations $\kappa = a + bt + ct^2$, where t is the temperature in °C; the parameters a, b, and c are given in Table 3. This is presumably because the Fe ionic complex species increases with increasing amounts of $FeCl_3$, which also causes an increase in the ionic interaction and the viscosities [5].

In the molten system $AlCl_3$-$DMSO_2$, the Raman spectra show that complex ions of Al-containing species were present in the $DMSO_2$-based melts [12]. Assume that a solvent reaction occurs for molten $AlCl_3$-$DMSO_2$ and $ZnCl_2$-$DMSO_2$. Then both melts were generally supposed in following equilibrium:

$$4AlCl_3 + n(CH_3)_2SO_2 = 3AlCl_4{}^- + Al[(CH_3)_2SO_2]_n{}^{3+}, \quad (1)$$

$$2ZnCl_2 + n(CH_3)_2SO_2 = ZnCl_4{}^{2-} + Zn[(CH_3)_2SO_2]_n{}^{2+}. \quad (2)$$

The formation of $AlCl_4{}^-$, $ZnCl_4{}^{2-}$, $Al[(CH_3)_2SO_2]_n{}^{3+}$ and $Zn[(CH_3)_2SO_2]_n{}^{2+}$ was expected, where the $AlCl_4{}^-$ and $ZnCl_4{}^{2-}$ ions were stable compounds of tetrahedral coordination. However, if $FeCl_3$-$DMSO_2$ melts react similar to (1) and (2), some of the Fe ions will be present as complex cations in the present electrolyte systems. Therefore, in the case of $FeCl_3$-$DMSO_2$, the ionic reaction between $FeCl_3$ and $DMSO_2$ can be expressed as

$$4FeCl_3 + n(CH_3)_2SO_2 = 3FeCl_4{}^- + Fe[(CH_3)_2SO_2]_n{}^{3+}. \quad (3)$$

What kinds of Fe-containing species exist must depend on complex formation of higher coordination numbers. Non-complexing ionic species must be leading in transport properties such as ionic conductivity. It is also suggested that the information obtained from the spectra and the viscosity must be in parallel as to the ionic structure. The movement of ions increases with increasing temperature, and the conductivity was maximal for 30 mol% $FeCl_3$, as shown in Figure 4. The isotherms at 90 and 110 °C of the conductivity on changing the mole fraction of $DMSO_2$ in the systems $ZnCl_2$-$DMSO_2$ [5], $AlCl_3$-$DMSO_2$, and $FeCl_3$-$DMSO_2$ are shown in Figure 5. It is demonstrated that

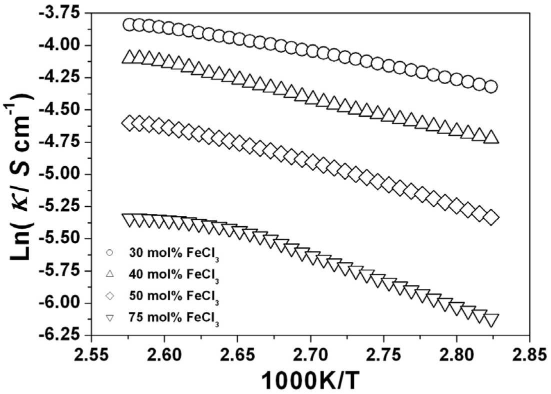

Fig. 6. Arrhenius plots of the electrical conductivity of molten mixtures of $FeCl_3$-$DMSO_2$ for 30, 40, 50, and 75 mol% $FeCl_3$.

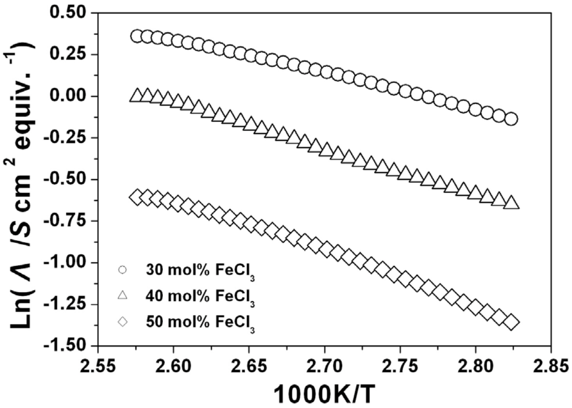

Fig. 7. Arrhenius plots of the equivalent conductivity of molten mixtures of $FeCl_3$-$DMSO_2$ for 30, 40, and 50 mol% $FeCl_3$.

the electrical conductivity increased with increasing mole fraction of $DMSO_2$ in the following ascending order $\kappa_{ZnCl_2-DMSO_2} < \kappa_{AlCl_3-DMSO_2} < \kappa_{FeCl_3-DMSO_2}$. These results indicate that the increase of $DMSO_2$ increases not only the molar volume but also the mobility of complex species.

The electrical and equivalent conductivities, fitted by the Arrhenius-type equations, $\kappa = \kappa_o \exp(-E_\kappa/RT)$ and $\Lambda = \Lambda_o \exp(-E_\Lambda/RT)$ for the $FeCl_3$-$DMSO_2$ melts, are shown in Figs. 6 and 7, respectively. The parameters of the activation energies for the isotherms of the electric conductivity and equivalent conductivity are given in Table 4. Generally, a molten salt with low lattice energy tends to show a high ionic migration, because low dissociation energy increases the number of free ions [3]. Thus, the 30 mol% $FeCl_3$ melt had the lowest electric conductivity activation energies among the investigated compositions. Both activation energies are closely linked and E_κ is always greater than E_Λ in the $FeCl_3$-$DMSO_2$ and $ZnCl_2$-$DMSO_2$ systems [5]. Similarity between E_κ and E_Λ is indicative of ionic packing or complex formation in the melt. In the $FeCl_3$-$DMSO_2$ system, the ratio of E_κ/E_Λ is about 1 – 2.5 at 81 – 115 °C.

Table 4. Activation energies of the conductivity and equivalent conductivity of molten $FeCl_3$-$DMSO_2$.

$FeCl_3$ mol%	$\kappa = \kappa_o \exp(-E_\kappa/RT)$ E_κ/kJ mol^{-1}	$\Lambda = \Lambda_o \exp(-E_\Lambda/RT)$ E_Λ/kJ mol^{-1}
30	16.52	8.63
40	22.17	22.94
50	25.26	25.92
75	28.22	–

4. Conclusions

The phase diagram of molten $FeCl_3$-$DMSO_2$ is given. The electric conductivity of $FeCl_3$-$DMSO_2$ melts has been measured at 30, 40, 50, and 75 mol% $FeCl_3$, and the density of $FeCl_3$-$DMSO_2$ melts has been measured at 20, 30, 40, and 50 mol% $FeCl_3$.

1. The electric conductivity was maximal, i.e. 0.02149 S/cm at 115 °C for 30 mol% of $FeCl_3$. The activation energies of electric conductivities and equivalent conductivity were 16.52 and 8.63 kJ/mol for E_κ and E_Λ, respectively.

2. The highest molar volume and the lowest density were shown by 20 mol% $FeCl_3$ at 81 – 115 °C. The density and molar volume could be influenced by the complex formation of the molecules or efficient packing of the ions.

3. The ionic migration of the four compositions in the $FeCl_3$-$DMSO_2$ system is in the order $30 > 40 > 50 > 75$ mol% $FeCl_3$.

Acknowledgement

This work was financially supported by the National Science Council, the Republic of China, under contract No. NSC 92-2214-E-224-008.

[1] S. Takahashi, N. Koura, S. Kohara, M. L. Saboungi, and L. A. Curtiss, Plasmas & Ions **2**, 91 (1999).
[2] Y. Zhao and T. J. VanderNoot, Electrochim. Acta **42**, 3 (1997).
[3] H. Y. Hsu and C. C. Yang, Z. Narturforsch. **56a**, 670 (2001).
[4] T. Hitato, J. Fransaer, and J. P. Celis, J. Electrochem. Soc. **148**, C280 (2001).
[5] M.-F. Shu, H.-Y. Hsu, and C. C. Yang, Z. Naturforsch. **58a**, 451 (2003).
[6] H. Y. Hsu and C. C. Yang, Z. Naturforsch. **58b**, 139 (2003).
[7] H. Y. Hsu and C. C. Yang, Z. Naturforsch. **58b**, 1055 (2003).
[8] C. C. Yang, T. H. Wu, and M. F. Shu, Z. Naturforsch. **59b**, 519 (2004).
[9] D. L. Thomas, J. Y. Cherng, and D. N. Bennion, J. Electrochem. Soc. **135**, 2674 (1988).
[10] G. P. Smith and G. F. Petersen, J. Chem. Eng. Data **6**, 493 (1961).
[11] J. Ye and Y. Sahai, Mat. Trans. JIM **37**, 170 (1996).
[12] L. Legrand, A. Tranchant, and R. Messina, Inorg. Chem. **35**, 1310 (1996).